Environmental Pollution 255 (2019) 113292

Contents lists available at ScienceDirect

Environmental Pollution

journal homepage: www.elsevier.com/locate/envpol

pH dependence of the binding interactions between humic acids and bisphenol A - A thermodynamic perspective☆

Li-hong Gan [a], Zi-run Yan [a], You-fei Ma [a], Yu-ying Zhu [a], Xiu-yan Li [a], Juan Xu [a, b, *], Wei Zhang [c]

[a] Shanghai Key Lab for Urban Ecological Processes and Eco-Restoration, Tiantong National Field Observation Station for Forest Ecosystem, School of Ecological and Environmental Sciences, East China Normal University, Shanghai, 200241, China
[b] Institute of Eco-Chongming (IEC), No. 20 Cuiniao Road, Chenjiazhen, Shanghai, 202162, China
[c] State Key Laboratory of Microbial Metabolism, School of Life Sciences and Biotechnology, Shanghai Jiao Tong University, Shanghai, 200240, China

ARTICLE INFO

Article history:
Received 2 July 2019
Received in revised form
27 August 2019
Accepted 19 September 2019
Available online 20 September 2019

Keywords:
Bisphenol A
Humic acids
Interaction
pH
Thermodynamic mechanism

ABSTRACT

The wide application of bisphenol A (BPA) leads to the emergence of BPA residuals in natural water environments. Dissolved organic matter (DOM) existed in water can bind with BPA, hence influencing the migration and transformation of BPA in aquatic environments. pH is a crucial factor governing the binding interactions between DOM and BPA. However, the mechanisms driven the binding process under different pH conditions are still unclear. In this study, the interactions between BPA and humic acids (HA), a primary component of DOM, are investigated over a wide pH range of 3–12 by integrating fluorescence quenching, dynamic light scattering and microcalorimetry. pH dependence of the binding interactions between HA and BPA are interpreted from a thermodynamic perspective. The results indicate that HA can spontaneously interact with BPA to form a stable HA-BPA complex. With the increasing pH, the binding interactions change from entropy driven to entropy-enthalpy co-driven. Hydrophobic force dominate the binding interactions under acidic condition. The synergy of hydrophobic force and hydrogen bond promotes the binding process under neutral condition. Under alkaline conditions, electrostatic repulsion participates the binding process in addition to hydrophobic force and hydrogen bond, weakening the binding strength. Therefore, neutral pH is favorable for HA to bind with BPA, consequently enhancing the dissolution of BPA in natural water bodies. The results are beneficial to better understand the pH dependent distribution of BPA in aquatic environments.

© 2019 Elsevier Ltd. All rights reserved.

1. Introduction

Endocrine disrupting chemicals (EDCs) bring about adverse impact on human health via intimating hormones or blocking receptor sites to disrupt basic physiological function (Komesli et al., 2015; Omar et al., 2016). Bisphenol A (BPA) is a typical EDC, which has toxic effects on male reproduction function even under trace amount of exposure (Manfo et al., 2014). The wide application of BPA in industrial production leads to the emergence of BPA residuals in natural water environments (Huang et al., 2012; Santhi et al., 2012).

Dissolved organic matter (DOM) ubiquitously exists in aquatic environments, comprising multiple aromatic and aliphatic hydrocarbon structures (Liu et al., 2017). DOM extensively participates the migration and transformation of contaminants in water environments, such as binding with hydrophobic organics to form complex (Zhu et al., 2012). This process markedly enhances the dissolution of the hydrophobic organic contaminants in water bodies (Song et al., 2017). BPA is moderately hydrophobic and is readily bound with DOM as well (Petrie et al., 2019). The binding interactions between DOM and BPA significantly influence the migration and transformation of BPA in aquatic environments (Bhatnagar and Anastopoulos, 2017).

Several mechanisms make contributions to the binding interactions between DOM and BPA such as hydrogen bond, aromatic stacking, hydrophobic force, and electrostatic interaction (Zhu et al., 2012). Hydrogen bond tends to be formed between DOM

☆ This paper has been recommended for acceptance by Dr. Sarah Harmon.

* Corresponding author. Shanghai Key Lab for Urban Ecological Processes and Eco-Restoration, Tiantong National Field Observation Station for Forest Ecosystem, School of Ecological and Environmental Sciences, East China Normal University, Shanghai, 200241, China.
E-mail address: jxu@des.ecnu.edu.cn (J. Xu).

https://doi.org/10.1016/j.envpol.2019.113292
0269-7491/© 2019 Elsevier Ltd. All rights reserved.

and organics carrying functional groups such as hydroxy and carboxyl. Aromatic stacking is likely to occur between DOM and organics with aromatic structures (Trout and Kubicki, 2007). Zhu et al. suggested that hydrogen bond is more significant than aromatic stacking for the interactions between DOM and BPA based on Gaussian calculation (Zhu et al., 2012). In addition, the inclusion of BPA into the cavity of cyclodextrins implies the existence of hydrophobic binding between BPA and DOM (Chelli et al., 2007). The binding interactions between BPA and DOM are highly correlated with solution conditions since hydrogen bond, aromatic stacking and hydrophobic interaction are evolving under different pHs, ionic strengths and temperatures. Especially, pH is a critical factor governing the interactions between DOM and contaminants (Casanova et al., 2018; Longstaffe et al., 2013). Carrying two phenol groups, BPA exists in three possible forms: molecular, mono-anion and dianion forms depending on solution pH (Qi et al., 2017). Simultaneously, the configuration of DOM is also distinct at different pH levels (Longstaffe et al., 2013; Saldana-Robles et al., 2018). However, previous investigations mainly focus on the binding affinity between DOM and contaminants under different pH conditions, deep insights into the binding mechanisms influenced by solution pH are still lacked.

In this study, the interactions between BPA and humic acid (HA), a primary component of DOM (Li and Hu, 2016; Wu et al., 2016), are investigated over a wide pH range of 3–12 by integrating fluorescence quenching, dynamic light scattering (DLS) and microcalorimetry. The binding affinity of the interactions are quantified, and the configuration changes of HA after binding with BPA are explored. This study aims to characterize the binding interactions between HA and BPA, and to interpret the mechanisms driven the binding process from the thermodynamic aspect. The results are beneficial to better understand the pH dependent migration and transformation of BPA in natural aquatic environments.

2. Materials and methods

2.1. Sample preparation

HA (No. 53680) and BPA (No. 239658) were purchased from Sigma-Aldrich Co. USA. Other reagents of analytical grad were from Sinopharm Chemical Reagent Co., China. To maintain the assigned pH during the binding experiments, 50 mM phosphate buffer (PBS) was used to prepare HA and BPA solutions to guarantee sufficient buffering capability. The stock solution of HA was filtered through a 0.45 μm membrane before utilization. The concentration of HA was quantified by total organic carbon (TOC) on multi N/C® 3100 analyzer (Analytik Jena, Germany), which was determined to be 2885 mg C/L.

2.2. Binding experiments between HA and BPA

BPA, HA and PBS were added into eight volumetric flasks, making the final concentration of HA to be 5 mg C/L. The concentrations of BPA in the flasks ranged from 0 to 28 mg/L with 4 mg/L increment. Three parallel samples were prepared for each BPA concentration. All the solutions were blended thoroughly and balanced for 4 h before fluorescence measurements. The binding interactions between HA and BPA were investigated under different temperatures (15, 25, 35 °C), pH (3–12), and ionic strengths (50–1000 mM). The solution pH was adjusted using 50 mM NaOH and 50 mM H_3PO_4, while ionic strength was adjusted with 1 M NaCl.

2.3. Spectral analysis

The fluorescence spectrum of HA-BPA mixture was collected on a luminescence spectrometer (F-4600, Hitachi Co., Japan). The excitation wavelength was set at 270 nm, and emission wavelength ranged from 300 to 550 nm at 0.2 nm increment. The excitation/emission slits were both 5 nm, and the scan speed was 240 nm/min. The UV–Vis spectra of HA-BPA mixture was measured on a spectrophotometer (UV-4500, Shimadzu Co., Japan). Fourier transform infrared spectroscopy (FTIR) was employed to characterize the functional groups of HA before and after the binding interactions (Nicolet iS5, Thermo Co., USA).

2.4. Isothermal titration calorimetry (ITC) measurement

Microcalorimetry (ITC-200, MicroCal Co., USA) was applied to obtain the thermodynamic parameters of the interactions between HA and BPA. HA (476.60 mg C/L) and BPA (423.03 mg/L) were prepared in 50 mM PBS (pH 9.5) and degassed for 15 min under vacuum. Here, ITC measurement was only conducted at pH 9.5, as the ITC signals were too weak to analyze at pH 5 and 7. High concentrations of BPA and HA were utilized for a better resolution of the signals in heat change, since the binding affinity were independent of HA and BPA concentrations (Yan et al., 2019b). BPA was injected into PBS buffer and HA solution, respectively. The working volume of the titration cell was 199.3 μL. An initial equilibrium time of 90 s was required before 19 injections. Each titration was completed by injecting 2 μL BPA into the working cell in 4 s, with 120 s spacing time between injections. Temperature was regulated at 25 °C and the stirring rate was 750 rpm. Data was analyzed by Origin 8.0 (Yan et al., 2019b), as described in Supplementary Materials.

2.5. Other analysis

Zeta potential and hydrodynamic radius (R_h) of HA before and after binding with BPA were measured by DLS (NANO ZS3600, Malvern Co., UK). Each sample was measured in triplicate at 25 °C.

3. Results and discussion

3.1. Complex formation between HA and BPA

The fluorescence of HA was quenched by BPA (Fig. 1) for two possible mechanisms: static quenching due to the formation of HA-

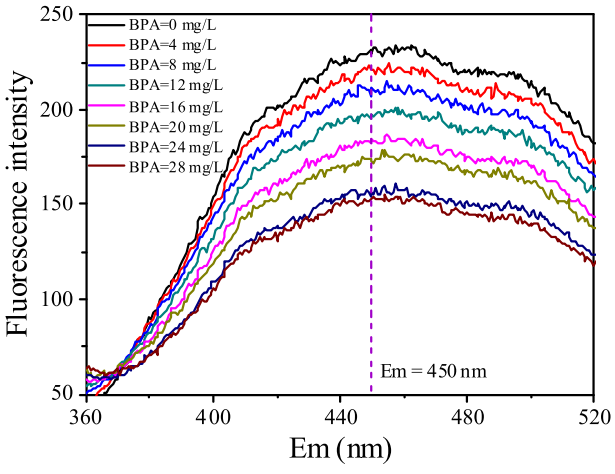

Fig. 1. The fluorescence of HA quenched by increasing BPA dosage (pH 7, ionic strength 50 mM, 25 °C).

BPA complex at ground state, and dynamic quenching arising from the molecular collision at excited state (Xu et al., 2013). Sterne-Vomer equation could verify the quenching mechanisms (Yu et al., 2015):

$$\frac{F_0}{F} = 1 + K_q \tau_0 [Q] \quad (1)$$

Where F and F_0 are the fluorescence intensity of HA (Ex/Em 270/450) with and without BPA addition; τ_0 is the average lifetime of HA, whose value is 10^{-8} s (Yan et al., 2019a); [Q] is BPA concentration; K_q is the quenching rate constant. As shown in Table 1, the values of K_q were far larger than the maximum diffusion collision quenching rate constant of 2.0×10^{10} L/mol/s (Yan et al., 2019a), excluding the possibility of dynamic quenching. Accordingly, static quenching dominated the binding process with the formation of HA-BPA complex, that was also confirmed by UV–Vis difference spectrum in Fig. S1 (Xu et al., 2013).

The variation in FTIR spectra of HA also revealed the formation of HA-BPA complex (Fig. 2). Compared to pristine HA, the peaks ascribed to aliphatic C–H bending (2926 cm^{-1} and 2850 cm^{-1}) (Adeyinka and Moodley, 2019) and C=C stretching in aromatic rings (1585 cm^{-1}) (Tian et al., 2018) disappeared in HA-BPA complex. A new peak corresponding to C=O stretching of carboxylic acid groups (1714 cm^{-1}) was observed (Chen et al., 2015). The results revealed the configuration changes of HA after binding with BPA: the hydrophobic structures (such as aromatic rings and alkyl groups) were occupied by BPA, while the hydrophilic groups (such as carboxylic acid groups) were exposed. Accordingly, hydrophobic interactions might play crucial roles in the binding interactions between HA and BPA. In addition, the magnified peak intensity at 1264 cm^{-1} being related with C–O in carboxyl groups indicated the enhancement of hydrogen bond in HA-BPA complex (Wang et al., 2012).

3.2. pH dependence of the binding interactions between HA and BPA

The binding constant (K) and the number of binding sites (n) was determined as follows (Zhang et al., 2010):

$$log\frac{F_0 - F}{F} = logK + nlog[Q] \quad (2)$$

Table 1
Binding constant (K), binding site (n) and quenching rate constant (K_q) of the interactions between HA and BPA at various pH values (ionic strength 50 mM, temperature 25 °C).

pH	K ($\times 10^3$ L/mol)	n	R_2^2	K_q ($\times 10^{11}$ L/mol/s)	R_1^2
3	15.09 ± 0.51	1.19 ± 0.008	0.997	2.63 ± 0.08	0.982
4	5.76 ± 1.98	1.03 ± 0.04	0.955	4.03 ± 0.36	0.980
5	41.78 ± 7.44	1.20 ± 0.06	0.993	3.05 ± 0.12	0.968
6	30.63 ± 6.23	1.23 ± 0.03	0.965	3.29 ± 0.17	0.972
6.5	11.89 ± 1.45	1.12 ± 0.01	0.995	3.52 ± 0.13	0.991
7	361.51 ± 3.33	1.49 ± 0.004	0.998	4.68 ± 0.13	0.985
7.5	242.92 ± 14.47	1.47 ± 0.01	0.949	2.68 ± 0.02	0.974
8	94.47 ± 3.86	1.39 ± 0.003	0.992	2.44 ± 0.04	0.971
8.5	37.63 ± 7.89	1.27 ± 0.02	0.995	3.06 ± 0.13	0.984
9	10.24 ± 4.19	0.97 ± 0.23	0.960	3.01 ± 0.19	0.962
9.5	4.57 ± 0.26	1.04 ± 0.006	0.975	3.06 ± 0.07	0.972
10	2.80 ± 0.58	0.99 ± 0.02	0.960	2.91 ± 0.15	0.975
10.5	1.69 ± 0.56	0.93 ± 0.04	0.952	3.02 ± 0.04	0.967
11	1.04 ± 0.34	0.91 ± 0.03	0.953	2.10 ± 0.11	0.967
11.5	1.32 ± 0.17	0.89 ± 0.02	0.958	3.56 ± 0.31	0.955
12	1.08 ± 0.05	0.87 ± 0.006	0.953	3.42 ± 0.12	0.963

R_1 is the regression coefficient according to Eq. (1).
R_2 is the regression coefficient according to Eq. (2).

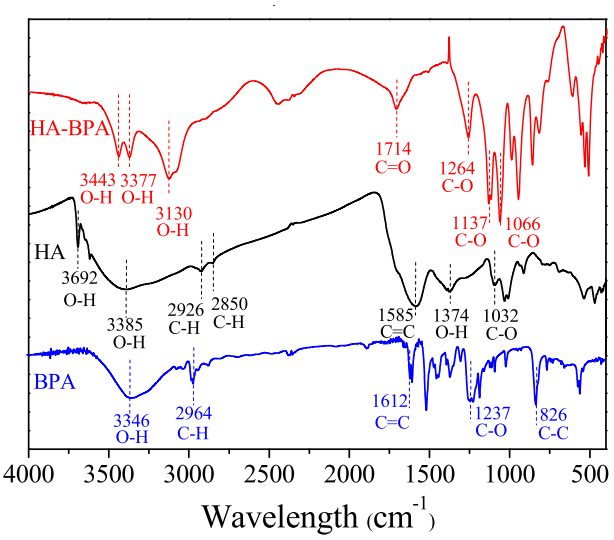

Fig. 2. FTIR spectra of HA before and after binding with BPA (pH 7, ionic strength 50 mM, 25 °C).

The binding constant (Table 1) changed along with the pH values, which could be divided into three regions (Fig. 3): (i) pH 3–6.5, the binding constant slightly fluctuated (Region 1); (ii) pH 7–9, the binding constant pronouncedly increased to a peak value of 3.6×10^5 L/mol at pH 7 and then monotonously decreased (Region 2); (iii) pH 9.5–12, the binding constant gradually decreased and maintained stable (Region 3).

In Region 1, the binding constant was relatively lower, ranging from 5.76×10^3 to 4.18×10^4 L/mol (Table 1). The weak binding affinity was related with the properties of HA and BPA under the acidic conditions. pH significantly affected the configuration of HA colloids. As showed in Fig. 4a, the size of HA was decreasing with the declining pH from 6.5 to 3. HA colloids were stabilized by weak forces such as electrostatic interaction, hydrophobic force and hydrogen bond. Hydrogen bond was progressively more important at a low pH. Strong intermolecular hydrogen bond held the HA molecules together, making HA colloids to be dense and compact (Wang et al., 2013). The decreasing R_h of HA with lowering pH also demonstrated the compression of HA molecules (Fig. 4a). The compressed configuration of HA colloids made some areas

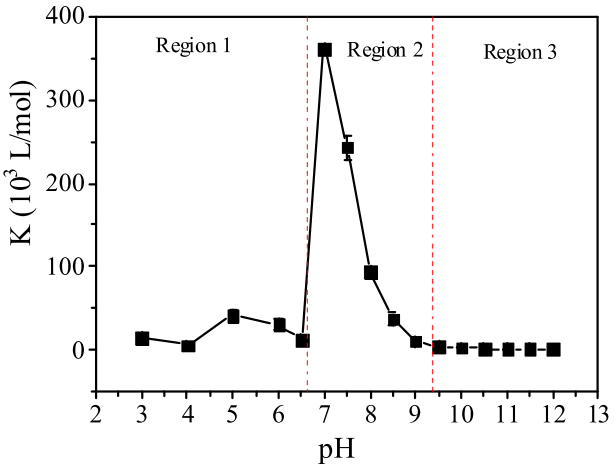

Fig. 3. Binding constant of the interactions between HA and BPA at different pH levels (ionic strength 50 mM, 25 °C).

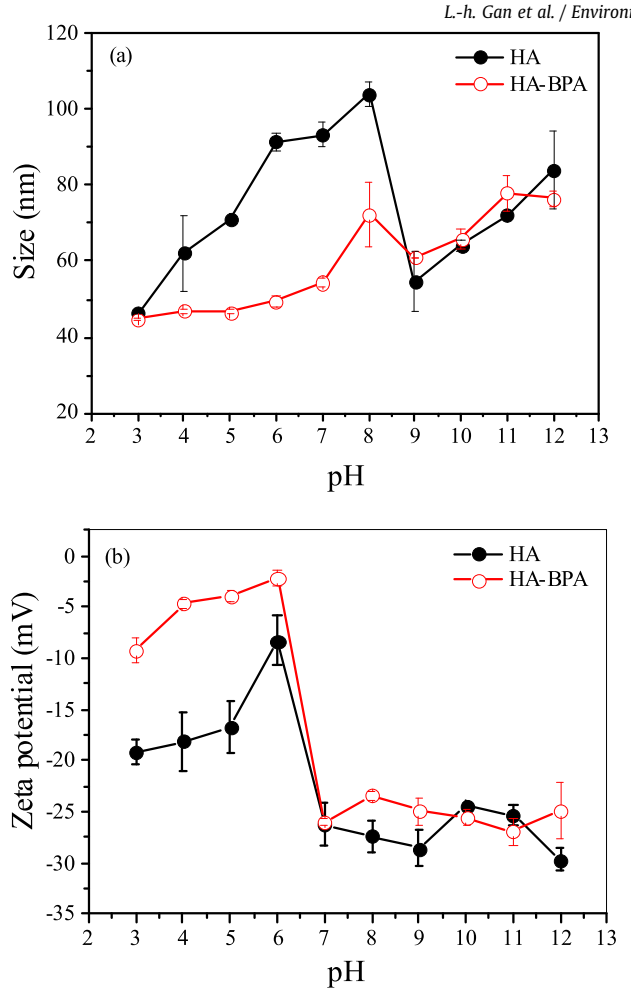

Fig. 4. Hydrodynamic radius (a) and zeta potential (b) of HA before and after binding with BPA at different pH values (ionic strength 50 mM, 25 °C).

inaccessible for BPA to bind with, impeding hydrophobic inclusion of BPA into HA. After binding with BPA, R_h of HA-BPA declined significantly, revealing the shrink of HA configuration. Simultaneously, zeta potential of HA-BPA increased after binding with BPA (Fig. 4b), indicating that the negative charges of HA decreased. Considering that BPA was in the molecular form in Region 1 (Fig. S2), the reduction in negative charges of HA were mainly ascribed to its conformations changes after binding with BPA rather than charges neutralization.

In Region 2, the peak value of binding constant appeared at pH 7 (Fig. 3), which was 1–2 magnitudes higher than those under acidic conditions (Table 1). Zeta potential of HA decreased to −27 mV at pH 7 and maintained stable at higher pH values (Fig. 4b). Two mechanisms might be responsible for the decreased zeta potential of HA: dissociation of acidic groups (such as −OH, −COOH) and breakage of internal hydrogen bonds in HA colloids (Klučáková and Věžníková, 2017). Both of the two processes would induce the expansion of HA configuration (Angelico et al., 2014), exposing more sites for BPA to bind with. Thus, the binding affinity between HA and BPA was significantly improved at pH 7. With the further increase in pH, the binding constant monotonously decreased (Fig. 3). That was because the increasing electrostatic repulsion between the negative charged HA and BPA in anion form impeded the binding process.

In Region 3, BPA existed in molecule, mono-anion and dianion forms (Fig. S2). The binding strength of BPA to HA was considered to be contributed by different BPA species, which could be distinguished by an empirical model (Figueroa et al., 2004). Over the pH range of 9.5–12, the apparent binding constant (K) is the composition of binding constants of three BPA species:

$$K = K^0\alpha^0 + K^-\alpha^- + K^{2-}\alpha^{2-} \quad (3)$$

Where K^0, K^-, K^{2-} are the binding constants of BPA in molecule, mono-anion and dianion forms to HA; α^0, α^-, α^{2-} are the proportions of BPA in molecule, mono-anion and dianion forms at a given pH value. As shown in Fig. S3, the binding constants of different BPA species to HA were fitted as K^0 (7.09×10^3 L/mol), K^- (2.11×10^3 L/mol), and K^{2-} (1.03×10^3 L/mol). The results indicated that both BPA molecules and anions contributed to the binding interactions in Region 3.

3.3. Mechanisms driving the binding processes between HA and BPA under different pH conditions

Thermodynamic parameters including Gibbs free energy change (ΔG), enthalpy change (ΔH), and entropy change (ΔS) indicated the mechanisms driven the binding interactions between HA and BPA. ΔH and ΔS at pH 5 and 7 were fitted by Van't Hoff Equation (Yan et al., 2019a).

$$\ln K = -\frac{\Delta H}{RT} + \frac{\Delta S}{R} \quad (4)$$

Where R is universal gas constant (8.314 J/mol/K), T is absolute temperature, and ΔG is calculated as:

$$\Delta G = \Delta H - T\Delta S \quad (5)$$

ITC measurement was conducted to obtain the thermodynamic parameters at pH 9.5 (Fig. S4). As summarized in Table 2, thermodynamic parameters were distinct under acidic, neutral and alkaline conditions, suggesting different binding mechanisms between HA and BPA in the three pH regions abovementioned. Hydrogen bond, hydrophobic force, and electrostatic interaction mainly contributed to the interactions between HA and BPA (Zhu et al., 2012): (1) hydrophobic force induced $\Delta H > 0$, $-T\Delta S < 0$; (2) hydrogen bond induced $\Delta H < 0$, $-T\Delta S > 0$; (3) electrostatic interaction induced $\Delta H \approx 0$, $-T\Delta S < 0$ (Ross and Subramanian, 1981).

Accordingly, the mechanisms of the binding interactions between HA and BPA at different pH levels could be identified from the thermodynamic parameters in Fig. 5. At pH 5, positive ΔH and negative -TΔS suggested the great contributions of hydrophobic forces. Considering that BPA carried no charges at pH 5 (Fig. S2), electrostatic interactions were excluded. Therefore, hydrophobic force mainly drove the binding interactions of HA and BPA under acidic conditions. At pH 9.5, negative ΔH indicated the prevalence of hydrogen bonds under alkaline conditions. The electrostatic repulsion between negative charged HA and BPA in anion form made -TΔS to be negative (Bi et al., 2014). The absolute value of ΔH was close to zero, indicating that the hydrophobic forces offset the negative ΔH produced by hydrogen bonds.

The highest binding strength presented at pH 7. Positive ΔH and negative -TΔS suggested the dominance of hydrophobic forces, being similar with pH 5. However, the absolute values of ΔH and -TΔS decreased compared to those of pH 5, yielding a more negative value of ΔG. This was caused by hydrogen bonds formation between HA and BPA at pH 7, as shown in FTIR spectrum (Fig. 2). Since BPA molecules accounted for more than 99% at pH 7 (Fig. S2), the influences of electrostatic interactions on the binding process were negatable. Influences of ionic strength on the interactions between BPA and HA could further illuminate the binding mechanisms at pH 7. The binding constant decreased dramatically by two magnitudes

Table 2
Thermodynamic parameters of the interactions between HA and BPA at various pH values (ionic strength 50 mM).

pH	T (°C)	K (× 10^3 L/mol)	n	R^2	ΔG (kJ/mol)	ΔH (kJ/mol)	ΔS (J/mol/K)	-TΔS (kJ/mol)
5[a]	15	0.58 ± 0.04	0.80 ± 0.007	0.974	−16.67	174.60	663.78	−191.27
	25	41.78 ± 7.44	1.20 ± 0.06	0.993	−23.31			−197.91
	35	63.05 ± 6.06	1.31 ± 0.02	0.957	−29.95			−204.54
7[a]	15	45.96 ± 4.34	1.28 ± 0.01	0.960	−25.84	136.50	563.39	−162.34
	25	361.51 ± 3.33	1.49 ± 0.004	0.998	−31.47			−167.97
	35	1849.11 ± 14.69	1.71 ± 0.002	0.983	−37.11			−173.61
9.5[b]	25	4.09		0.975	−20.60	−10.40	34.29	−10.39

R is the regression coefficient according to Eq. (2).
[a] Thermodynamic parameters obtained from Van't Hoff Equation.
[b] Thermodynamic parameters obtained from ITC measurement.

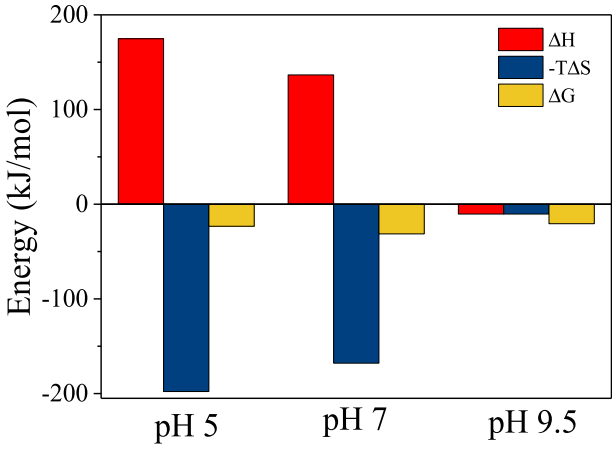

Fig. 5. Evolution of thermodynamic mechanisms driving BPA binding to HA at different pH values (ionic strength 50 mM, 25 °C).

when ionic strength increased from 50 to 500 mM (Table 3). High ionic strength clearly hindered the binding process of BPA to HA, that was highly related with the configuration changes of HA colloids as shown in Fig. S5a. HA molecules are stretched when ionic strength was 50 mM, with a high R_h value of 93.4 nm. Accordingly, more binding sites were exposed for BPA to bind with and a relatively higher binding constant was obtained. Increasing ionic strength from 50 to 500 mM compressed the electric double layer of HA colloids, as demonstrated by the increased zeta potential of HA (Fig. S5b). The configuration of HA became constrictive at high ionic strength of 500 mM, with a decreasing Rh value. That was not favorable for the binding interactions since less binding sites of HA were accessible for BPA. Further improving ionic strength to 1000 mM insignificantly altered the binding constant (Table 3). However, the binding behavior of BPA to HA totally changed, since zeta potential of HA was positive at ionic strength of 1000 mM. This was because the configuration of HA was altered by the extremely high ionic strength. Multiple Na^+ entered the interior of HA and bound with carboxyl and hydroxyl groups (Baker and Khahli, 2003), destroying the instinct structure of HA. R_h of HA was higher at ionic strength of 1000 mM than that at 500 mM, indicating that the reconstructed HA colloids presented in stretched state. It was noticed that the binding constants at ionic strength of 500 mM and 1000 mM were similar, although HA changed from negative charged to positive charged (Fig. S5b). This result also confirmed that electrostatic force was insignificant for the binding interactions between HA and BPA at pH 7. The synergy of hydrophobic force and hydrogen bond promoted the binding process, resulting in the highest binding affinity at the neutral condition.

Table 3
Binding constant (K) and binding site (n) of the interactions between HA and BPA at various ionic strengths (temperature 25 °C, pH 7).

Ionic strength (mM)	K (× 10^3 L/mol)	n	R^2
50	361.51 ± 3.33	1.49 ± 0.003	0.998
250	56.67 ± 0.74	1.29 ± 0.02	0.996
500	6.53 ± 0.66	1.05 ± 0.02	0.994
1000	6.0 ± 2.8	1.04 ± 0.05	0.998

R is the regression coefficient according to Eq. (2).

3.4. Environmental implication

The interactions between HA and BPA highly depended on solution pH. Neutral pH was favorable for HA to bind with BPA, that could markedly enhance the dissolution of BPA in natural aquatic environments. When solution pH changed, BPA would dissociate from HA-BPA complex, arising the risk of BPA re-releasing into the environments. This study implied that the BPA concentrations detected in natural water bodies were likely underestimated, since considerable BPA presented in the form of HA-BPA complex.

Actually, in addition to pH, other factors such as temperature, surfactants and aquatic colloids also influenced the binding interactions between HA and BPA. The binding strength of BPA to HA was clearly enhanced with the augment of temperature. Cationic surfactants were readily adsorbed by HA, hence promoted the binding interactions between BPA and HA due to the increased binding sites (Gao et al., 2001). Anionic surfactants increased the solubility of BPA in water phase and reduced the distribution of BPA in HA (Sanchez-Martin et al., 2003). Colloids such as bacteria, sand, clay were also important carriers of organic pollutants (Zhou et al., 2007), that weakened the stability of HA-BPA complex by competitive coordination with BPA. The interferes of these factors would definitely affect the distribution of BPA in natural water environments.

4. Conclusions

pH affected the configuration of HA, speciation of BPA, and hence the binding interactions between HA and BPA. The thermodynamic mechanisms for the binding interactions changed from entropy driven to entropy-enthalpy co-driven with increasing pH values (Fig. 6). Under acidic conditions, hydrophobic force dominated the binding interactions. The synergy of hydrophobic force and hydrogen bond strengthened the binding affinity under neutral condition. Under alkaline conditions, the integration of hydrophobic force, hydrogen bond and electrostatic repulsion weakened the binding affinity. Neutral pH obviously favored the formation of HA-BPA complex, therefore improving the dissolution of BPA in natural aquatic environments. Therefore, the concentrations of BPA in water bodies were likely underestimated due to the formation of HA-BPA complex.

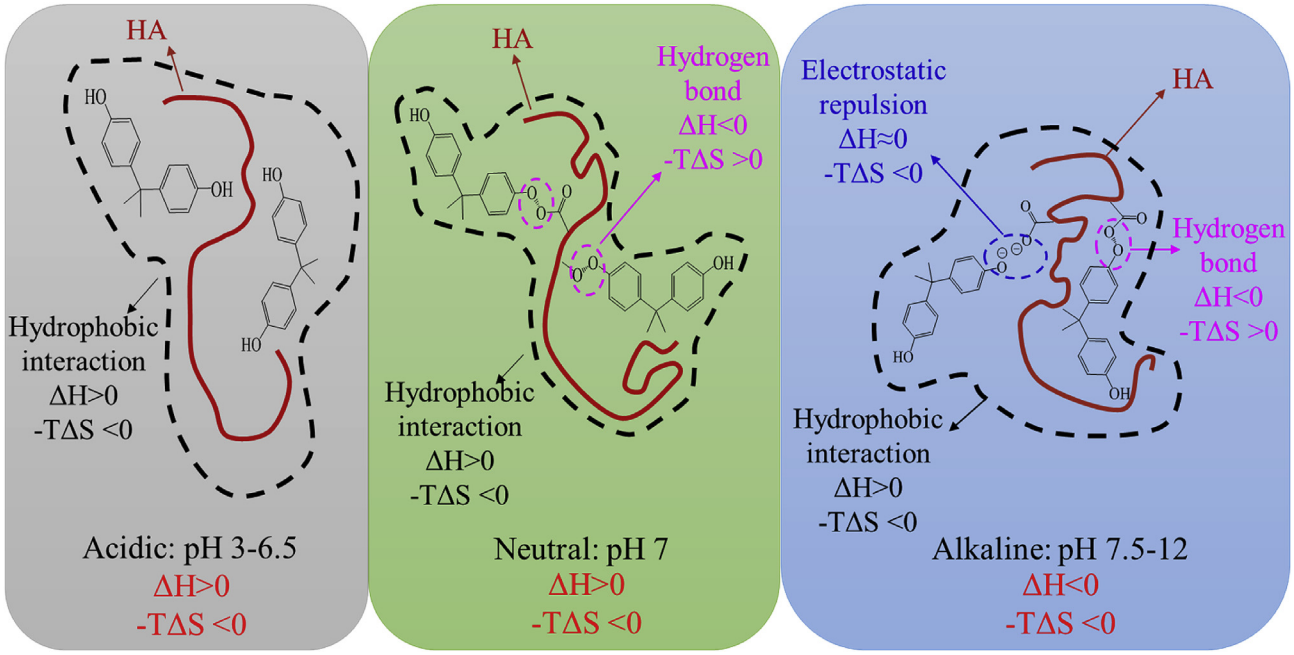

Fig. 6. The mechanisms of the interactions between HA and BPA under different pH conditions.

Acknowledgements

The authors wish to thank National Natural Science Foundation of China (51708224, 51978266), and the Core Facilities of the School of Life Sciences and Biotechnology in Shanghai Jiao Tong University for the support of this study.

Appendix A. Supplementary data

Supplementary data to this article can be found online at https://doi.org/10.1016/j.envpol.2019.113292.

References

Adeyinka, G.C., Moodley, B., 2019. Effect of aqueous concentration of humic acid on the sorption of polychlorinated biphenyls onto soil particle grain sizes. J. Soils Sediments 19, 1543–1553.
Angelico, R., Ceglie, A., He, J.Z., Liu, Y.R., Palumbo, G., Colombo, C., 2014. Particle size, charge and colloidal stability of humic acids coprecipitated with ferrihydrite. Chemosphere 99, 239–247.
Baker, H., Khahli, F., 2003. Comparative study of binding strengths and thermodynamic aspects of Cu(II) and Ni(II) with humic acid by Schubert's ion-exchange method. Anal. Chim. Acta 497, 235–248.
Bhatnagar, A., Anastopoulos, L., 2017. Adsorptive removal of bisphenol A (BPA) from aqueous solution: a review. Chemosphere 168, 885–902.
Bi, S., Pang, B., Wang, T., Zhao, T., Yu, W., 2014. Investigation on the interactions of clenbuterol to bovine serum albumin and lysozyme by molecular fluorescence technique. Spectrochim. Acta A 120, 456–461.
Casanova, F., Chapeau, A.L., Hamon, P., de Carvalho, A.F., Croguennec, T., Bouhallab, S., 2018. pH- and ionic strength-dependent interaction between cyanidin-3-O-glucoside and sodium caseinate. Food Chem. 267, 52–59.
Chelli, S., Majdoub, M., Trippe-Allard, G., Aeiyach, S., Chane-Ching, I., Jouini, M., 2007. Polyether-based polyrotaxane synthesis with controlled beta-cyclodextrin threading ratio. Polymer 48, 3612–3615.
Chen, W., Habibul, N., Liu, X.Y., Sheng, G.P., Yu, H.Q., 2015. FTIR and synchronous fluorescence heterospectral two-dimensional correlation analyses on the binding characteristics of copper onto dissolved organic matter. Environ. Sci. Technol. 49, 2052–2058.
Figueroa, R.A., Leonard, A., Mackay, A.A., 2004. Modeling tetracycline antibiotic sorption to clays. Environ. Sci. Technol. 38, 476–483.
Gao, B., Wang, X.R., Zhao, J.C., Sheng, G.Y., 2001. Sorption and cosorption of organic contaminant on surfactant-modified soils. Chemosphere 43, 1095–1102.
Huang, Y.Q., Wong, C.K.C., Zheng, J.S., Bouwman, H., Barra, R., Wahlstrom, B., Neretin, L., Wong, M.H., 2012. Bisphenol A (BPA) in China: a review of sources, environmental levels, and potential human health impacts. Environ. Int. 42, 91–99.
Klučáková, M., Věžníková, K., 2017. Micro-organization of humic acids in aqueous solutions. J. Mol. Struct. 1144, 33–40.
Komesli, O.T., Muz, M., Ak, M.S., Bakirdere, S., Gokcay, C.F., 2015. Occurrence, fate and removal of endocrine disrupting compounds (EDCs) in Turkish wastewater treatment plants. Chem. Eng. J. 277, 202–208.
Li, S., Hu, J., 2016. Photolytic and photocatalytic degradation of tetracycline: effect of humic acid on degradation kinetics and mechanisms. J. Hazard. Mater. 318, 134–144.
Liu, Chen, W., Qian, C., Yu, H.Q., 2017. Interaction between dissolved organic matter and long-chain ionic liquids: a microstructural and spectroscopic correlation study. Environ. Sci. Technol. 51, 4812–4820.
Longstaffe, J.G., Courtier-Murias, D., Simpson, A.J., 2013. The pH-dependence of organofluorine binding domain preference in dissolved humic acid. Chemosphere 90, 270–275.
Manfo, F.P.T., Jubendradass, R., Nantia, E.A., Moundipa, P.F., Mathur, P.P., 2014. Adverse effects of bisphenol a on male reproductive function. Rev. Environ. Contam. Toxicol. 228, 57–82.
Omar, T.F.T., Ahmad, A., Aris, A.Z., Yusoff, F.M., 2016. Endocrine disrupting compounds (EDCs) in environmental matrices: review of analytical strategies for pharmaceuticals, estrogenic hormones, and alkylphenol compounds. Trac. Trends Anal. Chem. 85, 241–259.
Petrie, B., Lopardo, L., Proctor, K., Youdan, J., Barden, R., Kasprzyk-Hordern, B., 2019. Assessment of bisphenol-A in the urban water cycle. Sci. Total Environ. 650, 900–907.
Qi, C., Liu, X., Lin, C., Zhang, H., Li, X., Ma, J., 2017. Activation of peroxymonosulfate by microwave irradiation for degradation of organic contaminants. Chem. Eng. J. 315, 201–209.
Ross, P.D., Subramanian, S., 1981. Thermodynamics of protein association reactions: forces contributing to stability. Biochemistry 20, 3096–3102.
Saldana-Robles, A., Damian-Ascencio, C.E., Guerra-Sanchez, R.J., Saldana-Robles, A.L., Saldana-Robles, N., Gallegos-Munoz, A., Cano-Andrade, S., 2018. Effects of the presence of organic matter on the removal of arsenic from groundwater. J. Clean. Prod. 183, 720–728.
Sanchez-Martin, M.J., Rodriguez-Cruz, M.S., Sanchez-Camazano, M., 2003. Study of the desorption of linuron from soils to water enhanced by the addition of an anionic surfactant to soil-water system. Water Res. 37, 3110–3117.
Santhi, V.A., Sakai, N., Ahmad, E.D., Mustafa, A.M., 2012. Occurrence of bisphenol A in surface water, drinking water and plasma from Malaysia with exposure assessment from consumption of drinking water. Sci. Total Environ. 427, 332–338.
Song, G., Li, Y., Hu, S., Li, G., Zhao, R., Sun, X., Xie, H., 2017. Photobleaching of chromophoric dissolved organic matter (CDOM) in the Yangtze River estuary: kinetics and effects of temperature, pH, and salinity. Environ. Sci. Proc. Imp. 19, 861–873.
Tian, X., Tian, C., Nie, Y., Dai, C., Yang, C., Tian, N., Zhou, Z., Li, Y., Wang, Y., 2018. Controlled synthesis of dandelion-like $NiCo_2O_4$ microspheres and their catalytic performance for peroxymonosulfate activation in humic acid degradation. Chem. Eng. J. 331, 144–151.
Trout, C.C., Kubicki, J.D., 2007. Molecular modeling of Al^{3+} and benzene interactions with Suwannee fulvic acid. Geochim. Cosmochim. Acta 71, 3859–3871.
Wang, L.F., Wang, L.L., Ye, X.D., Li, W.W., Ren, X.M., Sheng, G.-P., Yu, H.Q., Wang, X.K., 2013. Coagulation kinetics of humic aggregates in mono- and di-valent

electrolyte solutions. Environ. Sci. Technol. 47, 5042–5049.
Wang, L.L., Wang, L.F., Ren, X.M., Ye, X.D., Li, W.W., Yuan, S.J., Sun, M., Sheng, G.P., Yu, H.Q., Wang, X.K., 2012. pH dependence of structure and surface properties of microbial EPS. Environ. Sci. Technol. 46, 737–744.
Wu, W., Shan, G., Wang, S., Zhu, L., Yue, L., Xiang, Q., Zhang, Y., Li, Z., 2016. Environmentally relevant impacts of nano-TiO_2 on abiotic degradation of bisphenol A under sunlight irradiation. Environ. Pollut. 216, 166–172.
Xu, J., Sheng, G.-P., Ma, Y., Wang, L.F., Yu, H.-Q., 2013. Roles of extracellular polymeric substances (EPS) in the migration and removal of sulfamethazine in activated sludge system. Water Res. 47, 5298–5306.
Yan, Z.R., Meng, H.S., Yang, X.Y., Zhu, Y.Y., Li, X.Y., Xu, J., Sheng, G.P., 2019a. Insights into the interactions between triclosan (TCS) and extracellular polymeric substance (EPS) of activated sludge. J. Environ. Manag. 232, 219–225.
Yan, Z.R., Zhu, Y.Y., Meng, H.S., Wang, S.Y., Gan, L.H., Li, X.Y., Xu, J., Zhang, W., 2019b. Insights into thermodynamic mechanisms driving bisphenol A (BPA) binding to extracellular polymeric substances (EPS) of activated sludge. Sci. Total Environ. 677, 502–510.
Yu, X., Jiang, B., Liao, Z., Jiao, Y., Yi, P., 2015. Study on the interaction between Besifloxacin and bovine serum albumin by spectroscopic techniques. Spectrochim. Acta A 149, 116–121.
Zhang, G., Zhao, N., Hu, X., Tian, J., 2010. Interaction of alpinetin with bovine serum albumin: probing of the mechanism and binding site by spectroscopic methods. Spectrochim. Acta A 76, 410–417.
Zhou, J.L., Liu, R., Wilding, A., Hibberd, A., 2007. Sorption of selected endocrine disrupting chemicals to different aquatic colloids. Environ. Sci. Technol. 41, 206–213.
Zhu, F.D., Choo, K.H., Chang, H.S., Lee, B., 2012. Interaction of bisphenol A with dissolved organic matter in extractive and adsorptive removal processes. Chemosphere 87, 857–864.